Journal of Energy Storage 92 (2024) 112090

Contents lists available at ScienceDirect

Journal of Energy Storage

journal homepage: www.elsevier.com/locate/est

Research Papers

Effect of particle size on the thermal conductivity of organic phase change materials with expanded graphite

Elisangela Jesus D'Oliveira [a,*], Ulugbek Azimov [a], Sol-Carolina Costa Pereira [a,b], Khalid Lafdi [a,c]

[a] Department of Mechanical and Construction Engineering, Northumbria University at Newcastle, NE1 8STT, UK
[b] School of Computing, Engineering & the Built Environment, Edinburgh Napier University, EH10 5DT, UK
[c] Department of Chemical and Materials Engineering, University of Dayton, OH, USA

ARTICLE INFO

Keywords:
Thermal energy storage
Expanded graphite
Thermal conductivity
Low-temperature phase change material

ABSTRACT

Numerous studies have been conducted to enhance the thermal conductivity of phase change materials (PCMs) using various techniques. Among them, adding high-conductive particles, such as expanded graphite (EG). Nevertheless, in the published literature, there is limited information about the impact of particle sizes on the thermophysical properties of the PCM. This work aims to investigate the impact of two particle sizes of EG (20 and 200 μm) on three commercial PCMs, RT62HC, RT64HC and OM65, using different characterisation techniques, including differential scanning calorimetry (DSC), scanning electron microscopy (SEM), and thermal conductivity measurements. The results indicated that the thermal conductivity of PCMs increases by incorporating the high-conductive particles. The highest thermal conductivity enhancement (156 %) was obtained for the composite PCM based on RT62HC with 6 wt% of 200 μm EG. It could be highlighted that the solid thermal conductivity results are better with particles of 20 μm in paraffin (RT64HC) and with particles of 200 μm in fatty acids (RT62HC and OM65).

1. Introduction

Thermal energy storage (TES) has continuously attracted much attention in recent years, as it can help address the mismatch between energy demand and supply gap characteristic of renewable sources, making energy utilization more efficient [1,2]. Among TES, latent heat thermal energy storage (LHTES) using phase change materials (PCMs) is a promising alternative due to storing and releasing large amounts of heat when undergoing phase change transformation [3] in a narrow temperature range [4]. Due to storage capacity and low supercooling, some of the most widely studied types of PCMs are organic materials, such as paraffin-based and fatty acids [5]. However, their low thermal conductivity (0.16–0.20 W/(m·K)) limits the heat transfer rate during charging and discharging. Several studies focused on improving the thermal conductivity of PCMs [6–10] by adding high-conductivity carbon particles.

Expanded graphite (EG) possesses a porous structure, high thermal conductivity (around 2000 W/m K) and large surface area [11,12], which plays an essential role in their usage as additives for heat transfer enhancement of PCMs. There is ample evidence in the literature demonstrating a noteworthy enhancement in the thermal conductivity of PCMs, even when using low mass fractions of these particles, as indicated by references [13–17]. Furthermore, the impact of EG on thermal conductivity can vary significantly based on the specific geometrical configurations of the particles. Regrettably, only a limited number of published studies have explored the influence of particle size to gain a comprehensive understanding of its effects on the thermal properties of PCMs, as cited in references [18, 19].

Lu et al. [20] studied the preparation, characterisation and thermal properties of EG/paraffin (melting point of 62 °C) prepared by vacuum impregnation. The analysis included the influence of three different particle sizes, 835, 525 and 432 μm, on the thermal properties of the paraffin. The experimental results showed higher thermal conductivity for paraffin with 5 wt% of EG80, size 525 μm, 1.492 W/(m·K) compared with pure paraffin, 0.355 W/(m·K), with a 123 % enhancement. A study conducted by Wang et al. [21] studied the effects of graphite microstructure evolution on the anisotropic thermal conductivity of EG/paraffin composites (CPCMs). It was concluded that thermal conductivity anisotropy was found in the CPCMs. Experimental and numerical studies conducted by Cai et al. [11] on the thermal properties of EG/paraffin composites included microscopic geometry configuration, thermal conductivity and saturation sorption capacity of EG. The CPCMs in the study were prepared by melting and stirring the molten mixtures

---

* Corresponding author.
E-mail address: elisangela.doliveira@northumbria.ac.uk (E. Jesus D'Oliveira).

https://doi.org/10.1016/j.est.2024.112090
Received 2 November 2023; Received in revised form 16 April 2024; Accepted 12 May 2024

Nomenclature

D	diameter [μm]
ΔH_{PCM}	latent heat PCM [kJ/kg]
ΔH_{CPCM}	latent heat of CPCM [kJ/kg]
cp	specific heat [J/kg·K]
k	thermal conductivity [W/(m·K)]
L	length [m]
T_m	melting point [°C]
wt%	mass fractions [%]

Greek symbols

φ	percentage content of PCM
ρ	density [kg/m^3]

Abbreviations

CPCMs	composite phase change materials
DSC	differential scanning calorimetry
EG	expanded graphite
LHTES	latent heat thermal energy storage
PCM	phase change material
PMMA	polymethyl methacrylate
SA	surface area
TES	thermal energy storage

Table 1
Thermophysical properties of phase change materials reported by the suppliers.

PCMs	Density, ρ [kg/m^3]	Melting temp., T_m [°C]	Latent heat, ΔH_{PCM} [kJ/kg]	Thermal conductivity, k [W/m·K]	Specific heat, c_p [kJ/kg·K]	Manufacturer
RT62HC	850	62–63	230	0.20	2.00	Rubitherm
RT64HC	880	63–65	250	0.20	2.00	Rubitherm
OM65	924	65	183	0.19	2.83	PLUSS

Table 2
Expanded graphite powder physical properties reported by SIGRATHERM Carbon.

Graphite	Diameter [μm]	Density, ρ [kg/m^3]	Carbon content [%]	Moisture content [%]
GFG20	20	120	>95	<2
GFG200	200	100	>95	<2

for 6 h at 60 °C. The saturation capacity is a parameter used to evaluate the effects of the infiltration ratio of paraffin into EG pores; the EG had a V-shaped pore structure with a pore size of 10–100 μm with a very high specific surface area.

An et al. [22] prepared binary eutectic mixtures based on octadecanoic acid (C18-acid), octadecanol (C18-OH) and EG (mass fractions of 1, 3, 5, 7 and 9 wt%), using shear mixing and melting techniques. The CPCMs latent heat was between 135.2 and 143.5 J/g in the melting process, with a melting temperature rate between 45.5 and 47 °C. During crystallisation, the latent heat was between 149.0 and 189.6 J/g and solidification temperature rates between 37.1 and 37.8 °C. The EG incorporated into the binary mixture significantly enhanced the CPCMs thermal conductivity from 0.066 W/(m·K) to 3.38 W/(m·K), with an enhancement of 192.3 %. Sari and Karaipekli [13] prepared n-docosane absorbed into EG, with mass fractions 2, 4, 7 and 10 wt%. The thermal conductivity of the pure PCM and the CPCMs were measured as 0.22, 0.40, 0.52, 0.68 and 0.82 W/(m·K). Zhang et al. [23] prepared a ternary fatty acid eutectic mixture (capric-palmitic-stearic acid) with expanded graphite. The thermal stability and reliability tests showed the composite had excellent stability after 500 cycles, as no decomposition was observed. Later studies demonstrated that incorporating EG increased the thermal stability of the CPCMs, due to the flexible properties of the supporting material, and the chain mobility and the inhibiting degradation are reduced [24].

Although extensive research was carried out over the last decade on graphite-based additives, particularly in the field of PCMs there is a notable gap in the literature concerning a comparative analysis of thermal properties across different composites. This gap is especially evident in the case of different PCMs, such as paraffin and fatty acids, combined with similar sizes of EG. Previous works, including that of D'Oliveira et al. [25], discussed the importance of investigating different thermophysical properties and drawing comparisons, highlighting the discrepancies reported in results from other studies using similar materials and methods.

The novelty of the current work lies in its specific focus on characterizing organic CPCMs based on different medium-temperature organic PCMs, RT62HC, RT64HC and OM65, combined with two different sizes of EG (20 and 200 μm). The CPCMs prepared are for applications in domestic space and water heating systems, with melting temperatures between 62 and 65 °C. In this study, the mass fraction of the EG was limited to equal to 6 wt%, considering the effect of including high conductive particles on the reduction of latent heat capacity of the PCM.

The goal of this study is to explore and establish correlations between particle size and the improvements in thermal properties. The emphasis on investigating the combination of the different PCMs and EG sizes, along with the specific focus on applications in domestic heating systems, contributes to the novelty of the research in addressing a gap in the comparative analysis of thermal properties for these specific CPCMs.

2. Experimental

2.1. Materials selection

In this study, three commercial phase change materials were evaluated, RT62HC and RT64HC from Rubitherm, where RT64HC is a paraffin, and OM55 from PLUSS, where both RT62HC and OM65 are fatty acids. The evaluation involved the use of two different sizes of EG particles, 20–200 μm, sourced from SIGRATHERM Carbon with a purity over 95 %. No further treatment was done to EG particles, which the supplier had already expanded. The detailed information on the materials used in this study, provided by the suppliers, are reported in Tables 1 and 2.

2.2. Preparation of PCMs/EG composites

The preparation of the CPCM was carried out using a two-step method as it offers a better incorporation of the particles into the base PCM, as reported by many studies [26–28]. Firstly, 70 g of PCM in the solid state in a beaker was heated in a hot plate stirrer (IKATM RCT) at a constant temperature of 80 °C. Once the PCM was completely melted, 2, 4 and 6 wt% of EG were added to the beaker. The mixture was magnetically stirred for 30 min at the speed of 800 rpm, keeping the temperature at 80 °C and then the molten samples were sonicated in an ultrasonic bath (BANDELIN "Sonorex digitec") for 30 min at the same temperature to improve the dispersion of graphite particles in the liquid PCM. To evaluate the effect of adding the graphite particles, surfactants

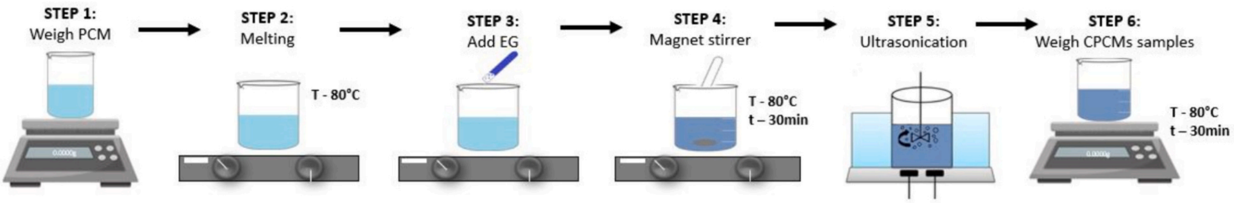

Fig. 1. Schematic of the preparation process of the CPCMs.

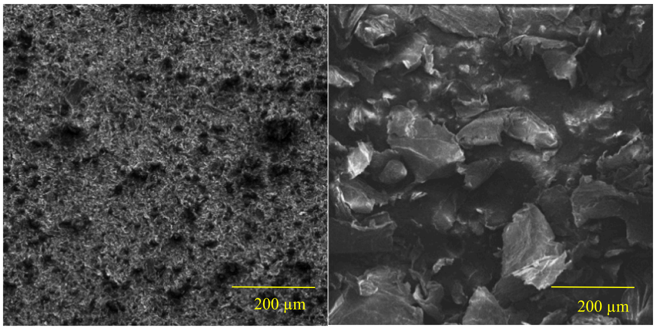

Fig. 2. SEM images of (a) GFG20 and (b) GFG200 with the same view field of 1.20 mm and an acceleration voltage of 5 kV.

or nucleating agents were not added to the mixture. Fig. 1 illustrates a complete schematic representation of the preparation of the CPCMs.

2.3. Characterisation

2.3.1. Scanning electron microscopy (SEM)

The microstructure of the prepared CPCMs was observed by using a scanning electron microscope instrument (SEM, TESCAN. MIRA3) at an accelerating voltage of 6 kV, and all the samples were platinum (Pt) coated with a thickness of 5 nm before observation to increase the electrical conductivity of the samples. The view field and magnification were varied between the two different EG sizes; for the CPCMs with the GFG20, a view field of 200 μm and magnification of 50 μm was adopted and for the CPCMs with the GFG200, a view field of 700 μm and magnification of 200 μm. The same view field allows a consistent and accurate comparison of the microstructure of the different samples, ensuring the reliability and validity of the data collected from the imaging analysis.

2.3.2. Differential scanning calorimetry (DSC)

The thermal parameters, such as the phase-change temperature, latent heat of melting and solidification, were determined using a differential scanning calorimetry instrument (DSC, 131 EVO Setaram). To measure the latent heat capacity and the phase change temperature, the scanning rate programme used at the DSC was 2 K/min and 10 K/min under a constant Argon atmosphere and a temperature programme of 15–90 °C. Aluminium crucibles (30 μl) were used for the reference and sample holder. The sample mass was controlled within 7–9 mg. Three samples of each composite were prepared, and each test was repeated three times for each sample to verify reproducibility; the average values were reported with the standard deviation.

2.3.3. Thermal conductivity equipment

The thermal conductivity of the solid samples was measured following the Transient Hot Bridge (THB) method using the THB-100 equipment from Linseis with a measurement accuracy of 5 %. The samples prepared were 50 mm × 25 mm with an average thickness of 5 mm. The Hotpoint sensor was placed between two solid block samples with flat and smooth surfaces, and a weight of about 2 kg was used to apply slight constant pressure for a controlled contact condition. The sensor can measure thermal conductivities ranging from 0.01 to 30 W/(m·K) and under a temperature range from −150 °C to 200 °C. Before the THB experiments, the Hotpoint sensor was single-point calibrated using polymethyl methacrylate (PMMA) as reference standard material, with a known thermal conductivity of 0.194 W/(m·K). Several measurements were taken for each sample, and the position of the sensor was changed each time. The thermal conductivity measurements were taken at 23 °C and the values reported are the average values from the repetitions.

2.3.4. Density

The density of the solid samples was measured using the Archimedes principles. This method is described in the BS EN ISO 1183-1 standard. The Ohaus density determination kit and a Fisherbrands balance with the uncertainty of (0.0001 g) were used. The displacement liquid was ethanol (purity 99.5 %) at a temperature of 20 °C. Samples were first weighed in the air (m_{air}) and then in ethanol (m_E). To reduce the errors associated with possible dissolution of PCM in the ethanol, the samples were measured again in the air. The temperature of the ethanol and air temperatures were measured. Efforts were made to ensure that no air bubbles were present in the ethanol during the weighing process, as this factor can compromise the accuracy of the measurement. The density (ρ) of the samples was provided by the following equation:

$$\rho = \left(\frac{m_{air}}{m_{air} - m_E}\right) \times (\rho_E - \rho_A) + \rho_A \tag{1}$$

where ρ_E and ρ_A is the density (in kg/m^3) of ethanol and air, respectively, and 0.1 MPa [Eq. 1]. Weighing the dry (and wet) sample before and after immersion in ethanol indicated that moisture uptake (or, in the case of wet samples, potential desorption) was negligible during the measurement. The density was measured for at least three samples. The average of the density for each substance is reported together with uncertainty.

As precision in density measurements is crucial, the utilization of ethanol allowed more sensitive and accurate measurements. To ensure the purity of the ethanol, the displacement liquid was changed regularly. This approach aimed to prevent any potential introduction of particles or residues from the PCMs and CPCMs, thereby maintaining the integrity of the density measurements.

3. Results and discussion

In this section, the experimental characterisation results are presented on the thermophysical properties of the PCMs and CPCMs.

3.1. Microstructural characterisation of composite phase change material

The SEM morphology microstructure of both EG and different CPCMs was obtained to investigate the infiltration of two particle sizes, EG-20 μm and EG-200 μm, with two fatty acids (RT62HC and OM65) and a paraffin wax (RT64HC). The images of the two different sizes of expanded graphite under the same view field and acceleration voltage, 1.20 mm and 5 kV, are shown in Fig. 2. It is observed that EG-200 μm exhibits a porous structure with a larger particle size than EG-20 μm.

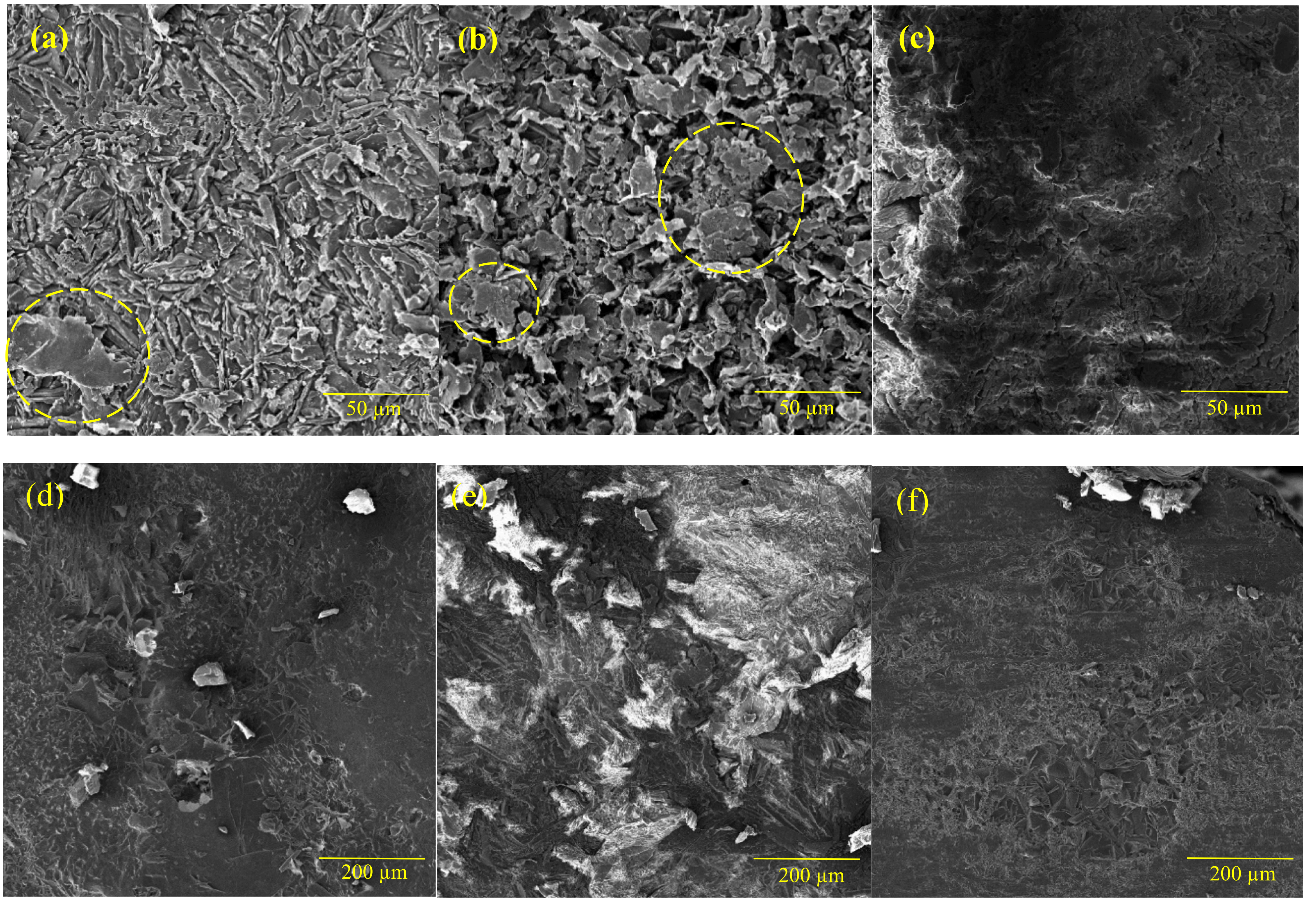

Fig. 3. SEM images of (a, b, c) RT62HC with 2, 4 and 6 wt% of 20GFG and (d, e, f) 200GFG.

Fig. 3a–c shows the morphology of the RT62HC with 2, 4 and 6 wt% of EG-20 μm; regardless of the particle size and concentration, the solid particles were well coated. There is no apparent issue of wettability between PCM and the carbon additives. Since the expanded graphite is anisotropic with lamellar morphology, after impregnation, the materials tend to pile up by laying down in xy direction. As the particle size is larger, the corresponding lamelaes are larger (Fig. 4).

Fig. 4a–c represents the morphology of the RT64HC with the different content of EG-20 μm. The RT64HC with 2 wt% of 20 μm exhibits good physical compatibility with the EG structure, having the paraffin confined within the EG pores. In Fig. 4b, it can be seen by the surface structure that the RT64HC was embedded into the EG matrices to enhance the microstructure of the CPCMs; the same can be observed in Fig. 4d–f of the RT64HC with 2, 4 and 6 wt% 200 μm. The paraffin was absorbed into large pores, and the gaps among the expanded graphite crystallised and aggregated into big particles, as can be seen in Fig. 4c shows some agglomerations of the particles (circled areas in Fig. 4c).

Fig. 5a–c shows the microstructure of the OM65 with a different loading of 20 μm and Fig. 5d–f with 200 μm. The PCMs, OM65 and RT64HC, are mixed with fatty acids; however, the morphology observed in Figs. 3 and 5 are entirely different. Further evaluation and deeper analysis of parameters such as wettability, surface tension, and saturation sorption capacity are required for composite PCMs with expanded graphite.

3.2. Latent heat and phase change temperature

The incorporation of highly conductive particles is a crucial step in enhancing the heat transfer rate of latent heat storage materials. In this section, using the DSC, the thermal properties of the prepared CPCMs were analysed, including onset melting/solidification temperature and the enthalpy of melting/solidification. The obtained endothermal and exothermal curves are shown in Fig. 6, and Table 3 presents the detailed data measured. The first cycle was discarded to eliminate the thermal history of the samples before the measurements; the consecutive cycles were used to calculate the average values and standard deviation to avoid discrepancies and outliers. Two heating and cooling rates were applied during DSC measurements, 2 K/min and 10 K/min. Some studies recommend using a scanning rate of 10 K/min to determine latent heat capacity, as this rate minimises errors. In contrast, a scanning rate of 2 K/min is suggested to obtain more accurate phase change transition values, specifically the onset temperature [29]. Table 3 summarises the average melting temperature, enthalpy values and standard deviation for the enthalpy at both heating rates.

It is expected that the addition of expanded graphite into the base PCM would reduce the latent heat capacity of the CPCMs because the expanded graphite does not suffer phase transformation at those temperatures. Theoretically, the latent heat of the composites is directly proportional to the PCM content and can be calculated with the following equation [30,31]:

$$\Delta H_{CPCM} = \varphi \Delta H_{PCM} \tag{2}$$

where ΔH_{CPCM} is the latent heat of CPCMs, φ is the percentage content of PCM, and ΔH_{PCM} is the latent heat of the PCM.

Table 3 shows that the melting enthalpies or latent heat for the OM65 is in good agreement with the data provided by the manufacturer, 182 kJ/kg and 183 kJ/kg. However, the measurements are not in good agreement with the data provided by the manufacturer of RT62HC and RT64HC, where the measured enthalpies are 198 kJ/kg and 223 kJ/kg, and the reported are 230 kJ/kg and 250 kJ/kg, approximated 30 kJ/kg

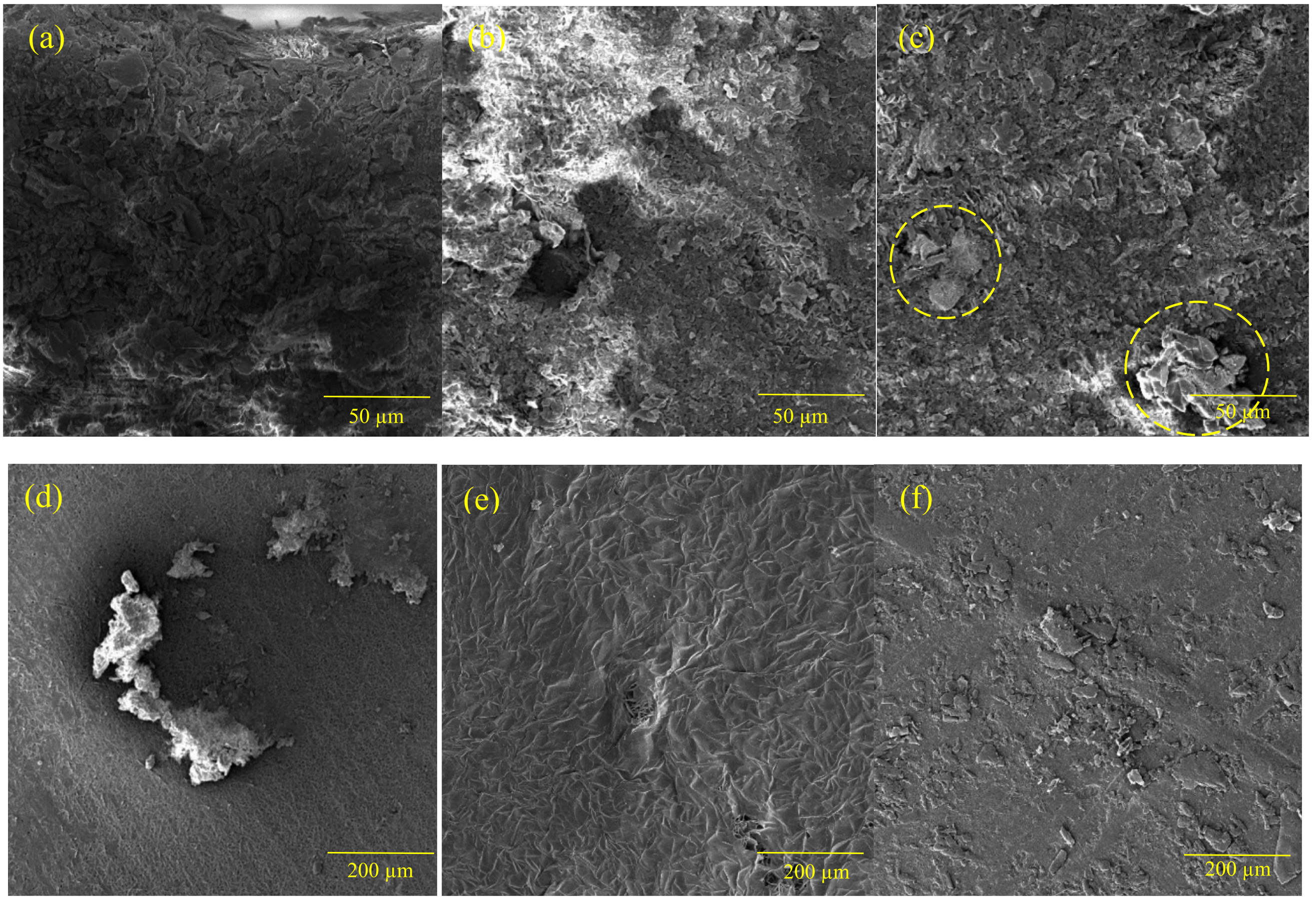

Fig. 4. SEM images of (a, b, c) RT64HC with 2, 4 and 6 wt% of 20GFG and (d, e, f) 200GFG.

lower. It is also observed that the heating rate significantly affects the results. For this reason, the procedure suggested by RAL-GZ 896 to identify the correct heating rate is recommended in further investigations.

From the average results shown in Table 3, it is evident that doping PCMs with EG decreases the latent heat capacity of the CPCMs in most of the cases. For instance, the CPCMs based on RT62HC with 20 μm GFG with mass fractions of 2, 4 and 6 wt% present a pseudo linear correlation; however, the diminution of latent heat double the expected at 2 K/min, 4 %, 7 % and 11 %, respectively. Therefore, no apparent correlation between the mass-weighted particles (wt%) and Eq. 2 has been identified. There have also been insignificant changes in the latent heat for the paraffin based PCM, RT64HC, with 200 μm GFG. Further analysis is required to discard inhomogeneities in the samples.

Fig. 6 shows the DSC curves for melting and solidification for the PCMs and 2 wt% composite PCMs with the evaluated EG particle sizes. The latent heat during melting of the pure RT62HC is 192.4 kJ/kg, and with the addition of 20 and 200 μm GFG, with mass fractions of 2, 4 and 6 wt%, the melting latent heats are 179.1, 175.9, 173.6, 170.5, 182.8 and 173.8 kJ/kg, respectively.

Fig. 6b presents the DSC curves for the composites with RT64HC as the base PCM. It shows more than one exothermal peak in the DSC curves, meaning there is more than one chemical composition. Fig. 6c presents the DSC curves of the composites PCMs with OM65. As anticipated, the endothermic and exothermic peaks of these Composite Phase Change Materials (CPCMs) exhibit a slight reduction in magnitude as the percentage of OM65 decreases. Additionally, it is noteworthy that the onset melting temperatures for all CPCMs have experienced a slight decrease with the introduction of both types of expanded graphite.

3.3. *Solid thermal conductivity*

Thermal conductivity significantly affects the heat transfer rate of LHTES; the significance in improving the thermal conductivity of PCMs was emphasised by many research papers [32,33], as this property is a crucial indicator of the performance of the storage material.

Fig. 7a shows the thermal conductivity enhancement ratio, and Fig. 7b shows the thermal conductivity of CPCMs different mass fractions of, 2, 4 and 6 wt%, of the two sizes of EG, 20 and 200 μm at room temperature (solid-state). It can be seen that the highest increase in thermal conductivity was for the CPCMs based on RT62HC with 200 μm GFG, with the mass fractions 2, 4 and 6 wt% being 0.320, 0.451 and 0.517 W/m·K, which had an enhancement of 58 %, 123 % and 156 %, respectively. The same behaviour can be seen for the CPCMs based on RT62HC with 20 μm GFG. The thermal conductivity enhancement with the fatty acid, RT62HC was the highest with both sizes of expanded graphite (20 and 200 μm GFG) when compared with the paraffin wax RT64HC and the fatty acid commercial bio-based OM65. Some studies indicate that the wettability of PCMs can play an important role [34], impacting the ability to absorb the EG. Also, organic PCMs based on fatty acids possess a higher wettability, when compared with paraffin wax-based PCMs and, therefore, are more likely to absorb and retain the EG, which leads to higher improvement in the thermal conductivity. However, in the results obtained, the OM65 is also a fatty acid but the average thermal conductivity enhancement is the lowest. The thermal conductivity of RT64HC with 200 μm GFG showed the lowest thermal enhancement when compared with the other CPCMs; with mass fractions of 2, 4 and 6 wt%, the thermal conductivity enhancement was 46 %, 70 % and 100 %, respectively. The CPCMs based on the latter demonstrated a different behaviour when compared with the CPCMs

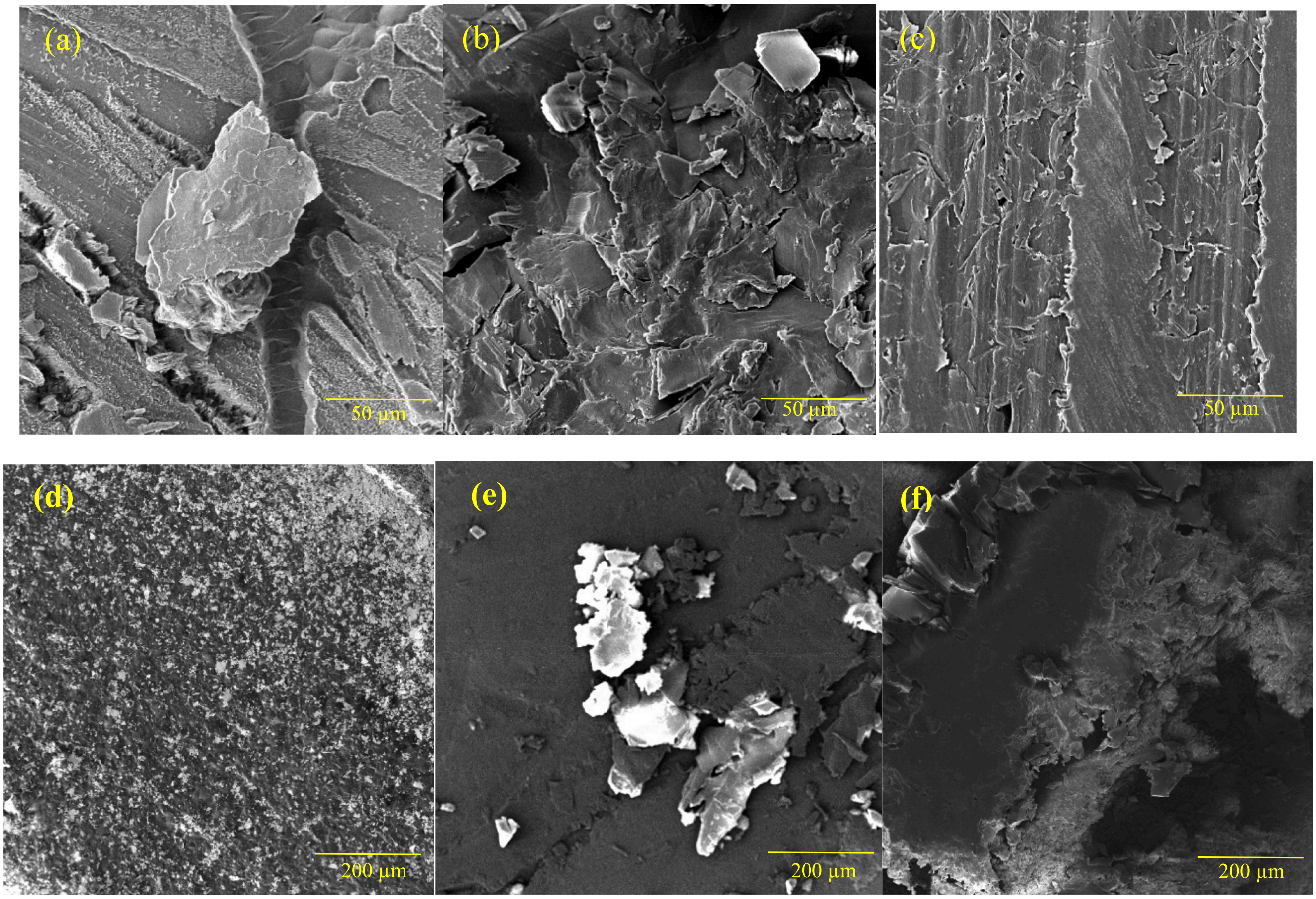

Fig. 5. SEM images of (a, b, c) OM65 with 2, 4 and 6 wt% of 20GFG and (d, e, f) 200GFG.

based on the RT62HC and OM65; for the case of the CPCMs based on the commercially available paraffin wax, RT64HC, the material prepared with the EG with the size of 20 µm had a more significant enhancement in the thermal conductivity when compared with the CPCMs prepared with 200 µm.

Fig. 7 shows that for both EG particle sizes, the solid thermal conductivity for the CPCMs studied increases linearly with the mass-weighted percentage (wt%) of EG particles. The thermal conductivity of the composites was fitted to a linear correlation.

Three correlations are proposed for the composites PCMs with EG, Eq. 3 for RT62HC, Eq. 4 for RT64HC and Eq. 5 for OM65.

$$k_s = 5.18x + 0.202 \tag{3}$$

$$k_s = 4.22x + 0.221 \tag{4}$$

$$k_s = 3.96x + 0.194 \tag{5}$$

The highest thermal conductivity enhancement (156 %) was obtained for the composite PCM based on RT62HC with 6 wt% of 200 µm EG. It could be highlighted that the solid thermal conductivity results are better with particles of 20 µm in paraffin and with particles of 200 µm in fatty acids.

3.4. Effects of density and mass fraction of EG

High density is desirable in thermal energy storage materials, as high density means higher volumetric storage heat capacity [35]. Fig. 8 presents the variation in density of the CPCMs with the increase of the mass fraction of the two sizes of EG, 20 and 200 µm, in the solid state. The physical properties of two high conductive particles are presented in Table 2, where the powder densities of 20 and 200 µm EG are 120 and 100 kg/m^3 (Fig. 9). Some studies concluded that the density of the composites has a substantial impact on the thermal conductivity [35]. In this study, there is no evidence of a correlation between the solid density and the thermal conductivity enhancement of the composite PCMs. For instance, CPCMs based on RT62HC with 20 µm EG were 956, 956 and 1010 kg/m^3, and the thermal conductivity increased accordingly 0.303, 0.421 and 0.465 W/(m·K), respectively. The CPCMs based on RT62HC with 200 µm EG was 962, 976 and 998 kg/m^3 and their thermal conductivity was 0.320, 0.451 and 0.518 W/(m·K), respectively [9].

3.5. Thermal stability

The long-term performance efficiency of LHTES depends on the stability and reliability of the storage material; therefore, charging and discharging cycling tests are fundamental [25]. This section presents the stability results of 10 cycles for some of the composite PCMs prepared. Fig. 10 shows the particle separation of the RT64HC with mass fractions of 2, 4 and 6 wt% of 20 µm EG after 10 heating and cooling cycles, leading to a clear separation between the base PCM and the EG particles. Although doping PCMs with EG particles could increase the thermal conductivity of PCMs without significant changes in the latent heat, a few cycles of the composite material reveal serious stability problems. Some papers reported that the addition of surfactants has a positive effect not only on the thermal stability of CPCMs but also on the latent heat capacity of the CPCM. For instance, Xin et al. [36] conducted an experimental characterisation of the thermal properties of an inorganic PCM, $Na_2HPO_4{\cdot}12H_2O$, with EG as their supporting material modified by CTAC, a cationic surfactant; the results showed that the ions of CTAC made a positive contribution to the endothermic process. To the best of

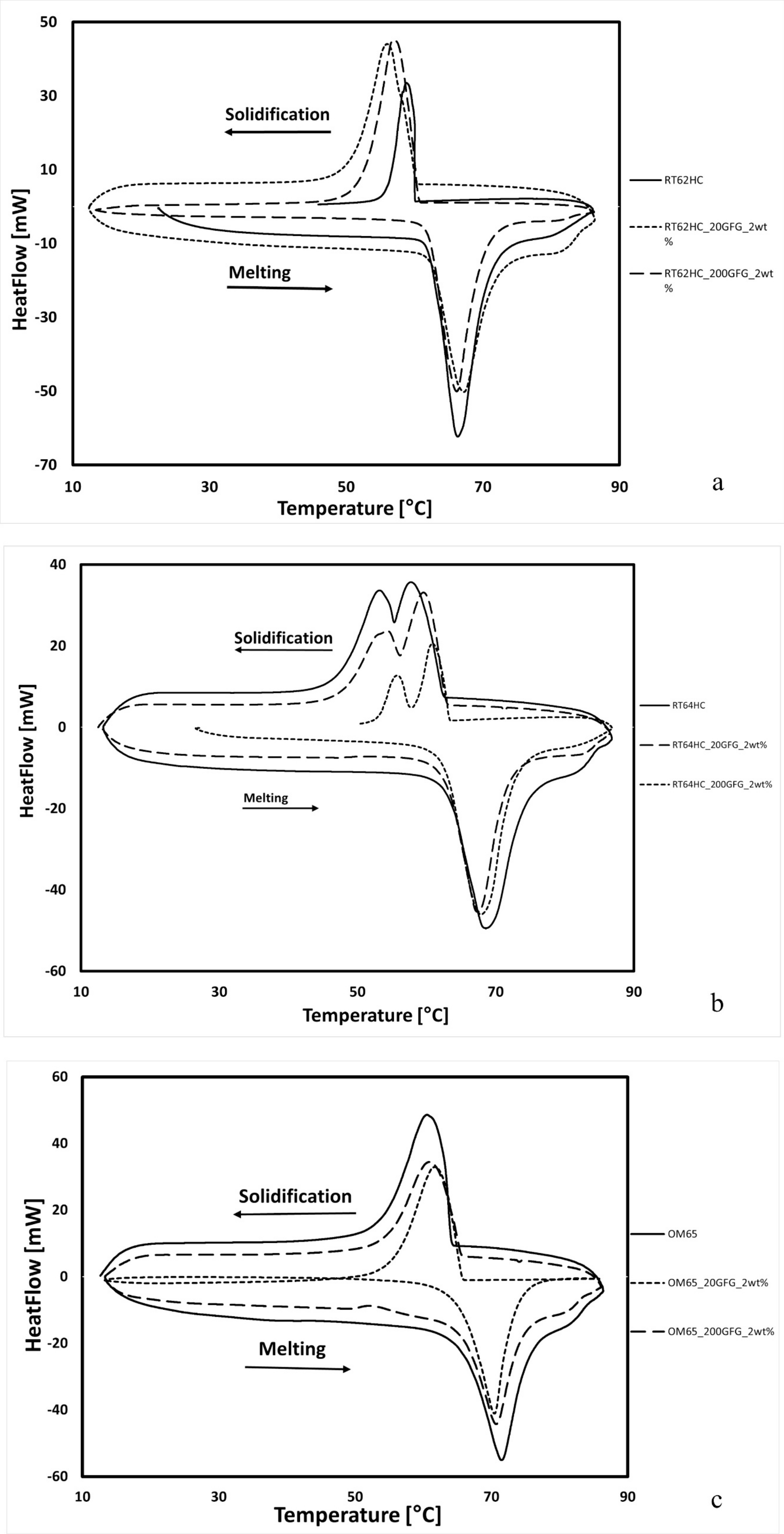

Fig. 6. DSC curves of RT62HC (a) RT64HC (b) and OM65 (c) and its composites with 2 wt% of 20 and 200 μm GFG.

Table 3
Measured thermophysical properties of CPCMs during Melting.

Material	wt %	Temp. @ 10 K/min [°C]	Enthalpy @ 10 K/min [kJ/kg]	Reduction @ 10 K/min [%]	Temp. @ 2 K/min [°C]	Enthalpy @ 2 K/min [kJ/kg]	Reduction @ 2 K/min [%]
RT62HC	0	62.4	192.4 ± 0.4	–	61.4	198 ± 3	–
GFG20	2	62.0	179 ± 5	7 %	61.6	190 ± 10	4 %
	4	62.3	176 ± 7	9 %	61.7	184 ± 7	7 %
	6	62.2	174 ± 3	10 %	62.0	175 ± 3	11 %
GFG200	2	62.2	171 ± 1	11 %	61.9	174 ± 1	12 %
	4	62.4	183 ± 1	5 %	61.5	186 ± 1	6 %
	6	61.8	174 ± 7	10 %	61.6	173 ± 13	13 %
RT64HC	0	62.8	217 ± 1	–	63.4	223 ± 7	–
GFG20	2	62.7	202.2 ± 0.4	7 %	62.8	206 ± 2	8 %
	4	62.4	205 ± 2	6 %	63.3	211 ± 4	5 %
	6	62.4	208 ± 6	4 %	61.9	208 ± 5	7 %
GFG200	2	62.6	220 ± 3	+ 1 %	63.0	226 ± 4	+ 1 %
	4	62.5	217 ± 7	0 %	62.6	211 ± 18	5 %
	6	62.9	207 ± 15	5 %	63.2	213 ± 19	4 %
OM65	0	65.6	177.3 ± 0.1	–	65.7	182 ± 5	–
GFG20	2	65.4	172 ± 3	3 %	65.1	178 ± 2	2 %
	4	65.4	169 ± 5	5 %	65.4	166 ± 16	8 %
	6	64.5	169 ± 2	5 %	64.4	164 ± 1	10 %
GFG200	2	65.0	172 ± 7	2 %	65.3	178 ± 4	2 %
	4	65.2	171 ± 6	8 %	65.2	176 ± 7	3 %
	6	64.4	164 ± 1	10 %	64.9	177 ± 16	3 %

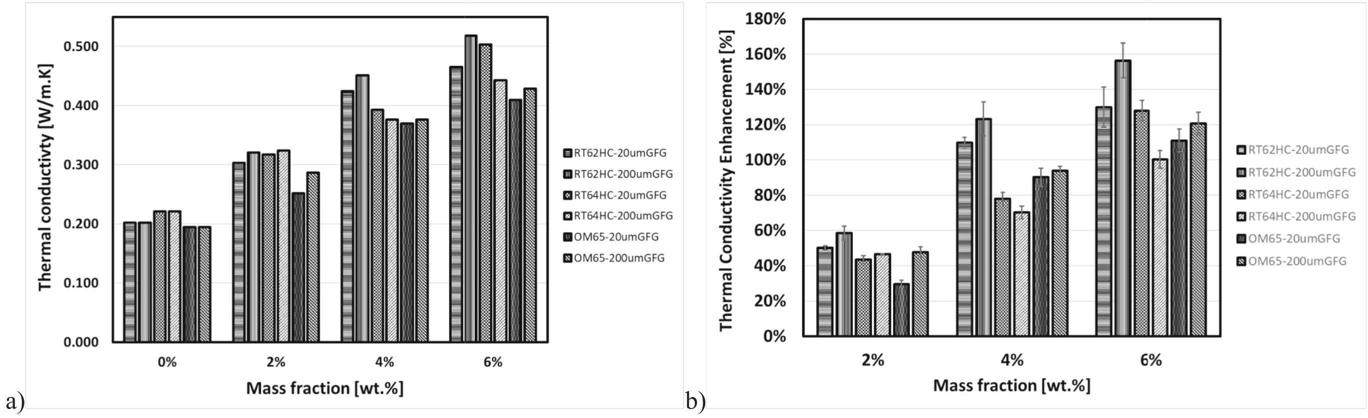

Fig. 7. Thermal conductivity values (a) and thermal conductivity enhancement ratio (b) of composite PCMs with different mass fractions of 20 and 200 μm GFG.

our knowledge, there is no systematic study or guideline about using surfactants with particles in PCMs in the available literature. Additional research is required to enhance the stability of PCM/EG composites, exploring alternative preparation methods like vacuum or the incorporation of different additives. Recently, Zhelezny et al. [37] proposed a new preparation method for shape-stable CPCM with paraffin wax and EG under vacuum conditions. The method aims to increase the penetration of paraffin in the porous structure of EG, reducing the air trapped and significantly enhancing the thermal conductivity of the composite.

3.6. Effects of EG on the properties of different PCMs

In this section, a comparison of the present results with the available literature using similar PCMs and EG particles is presented, focusing on the effects of mass fraction of different sizes of expanded graphite on the thermal conductivity of various organic PCMs (both paraffin waxes and fatty acids) with similar phase change temperature. Table 4 summarises relevant studies from the literature that have incorporated expanded graphite as a conductive filler to enhance the thermal conductivity of PCMs.

While the studies presented for comparison used similar materials, different treatment methods were applied to the expanded graphite that could result in variations in the measured properties, such as the thermal conductivity of the enhanced phase change materials and phase change behaviour.

Fig. 11 compares the thermal conductivity enhancement of the composites with the EG with the results obtained in this study. The compared results present significant differences in the enhancement of the thermal conductivity, Sarı and Karaipekli [10] reported 41 % enhancement for 5 wt%, while Fang et al. [37] reported 468 % with the same mass fraction of EG particles. The preparation of the CPCMs was similar to the preparation method implemented in the current study.

The variations in thermal conductivity measurements can be ascribed to several influencing factors. One possible factor is the type of graphite particle and its dispersion, as graphite can have different structures and properties, affecting the thermal conductivity enhancement. Additionally, the accuracy and precision of the equipment used may play a significant role, potentially affecting the results, particularly for measurements sensitive to temperature fluctuations, such as thermal conductivity and latent heat capacity. Even minor discrepancies in calibration can lead to disparities in recorded data. Hence, the precision and accuracy of the instruments stand as pivotal elements in achieving reliable results. Consequently, there is a pressing need for standardization in the methods and techniques employed to ensure consistency and accuracy in thermal conductivity assessments.

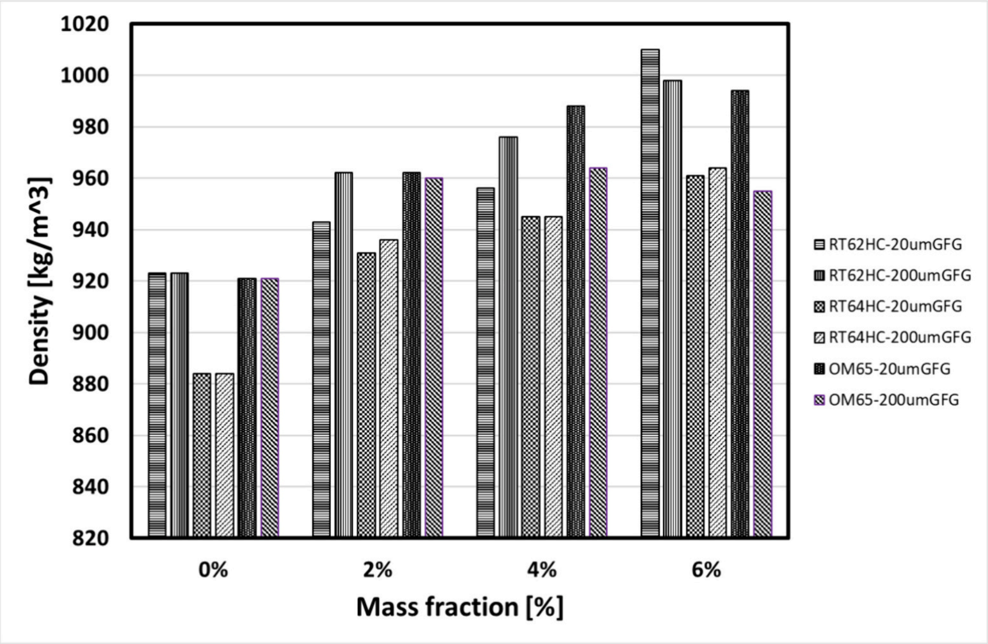

Fig. 8. Variation in density of the CPCMs with the addition of EG.

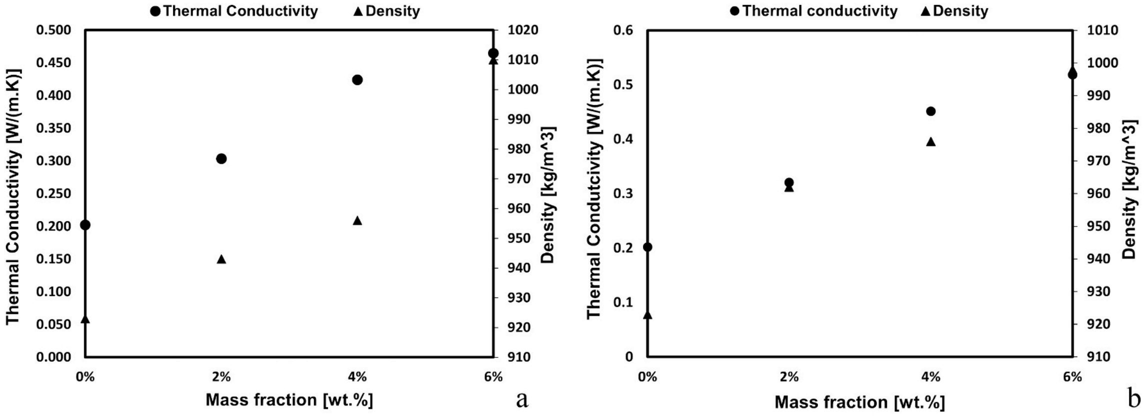

Fig. 9. Effects of mass fraction of 20 μm EG (a) and 200 μm EG (b) on the thermal conductivity and density of RT62HC.

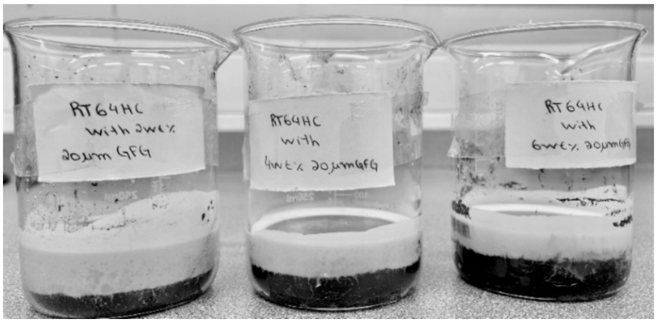

Fig. 10. Particle separation of RT64HC with mass fractions of 2, 4 and 6 wt% of 20 μm EG.

4. Conclusions

Low thermal conductivity is a primary limiting factor in using PCM in thermal energy storage applications. In this work, the thermal conductivity enhancement of three different organics PCMs with melting temperature range around 62 to 65 °C (RT62HC, RT64HC and OM65) doped with expanded graphite microparticles, was investigated for two sizes of particles, 20 and 200 μm, and three mass fractions concentrations. From the results obtained, the following conclusions were drawn:

- The addition of EG into the PCMs resulted in a significant improvement in the thermal conductivity of the CPCMs because of its effective conduction network. Measurements results indicated, that the thermal conductivities of the CPCMs ranged from 0.194 to 0.518 W/(m·K).
- The CPCMs that exhibited the most significant thermal conductivity enhancement were based on the RT62HC with 6 wt% of 200 μm EG, 0.518 W/(m·K), with an enhancement of 156 % compared with the pure RT62HC, 0.202 W/(m·K).
- Despite the enhancement in thermal conductivity enhancement for the CPCMs, there is a clear phase separation during the first thermal cycles. Thermal stability is still a limiting factor for the CPCMs.
- As expected, adding EG to PCMs reduces their latent heat storage capacity due to the decreased total PCM mass. DSC analysis showed a maximum −13 % decrease in the latent heat of melting for CPCMs

Table 4
A summary of recent studies that used expanded graphite as a conductive filler.

Base PCM			Conductive filler		Enhanced PCM				Ref.
PCM/T_m [°C]	k_{solid} [W/(m·K)]	ΔH [kJ/kg]	Parameters	Preparation	Mass fraction [wt%]	k_{solid} [W/(m·K)]	k enhancement [%]	ΔH [kJ/kg]	
Paraffin/ [53–57]	0.258	119.32	Size: 200–1200 μm	Supplied by: LKAB Minerals Ltd. EG was subjected to microwave treatment.	2	0.53	105 %	113.8	[16]
					4	0.788	205 %	111.7	
					6	0.977	279 %	113.3	
			Size: 50–200 μm		2	0.565	119 %	147.1	
					4	0.903	250 %	139.7	
					6	1.263	390 %	141.8	
Paraffin/ [58.2 °C]	0.309	151.6	D: 15 to 400 μm SA: 42.53 m^2/g	Supplied by Qingdao Tiashendgda Graphite CO. EG was dried using a drying oven at 70 °C for 12 h.	0.5	0.371	20 %	156.7	[38]
					1	0.532	72 %	158.9	
					2	0.855	177 %	154.2	
					3	1.217	294 %	147.2	
					4	2.3	644 %	138	
Paraffin/ [58–60 °C]	0.28	–	Size: 300 μm Expansion coefficient: 200 ml/g	Supplied by Qingdao Graphite Co. EG was obtained by rapid expansion and exfoliation	2	0.99	254 %	138.0	[2]
					5	1.59	468 %	134.8	
					10	4.45	1489 %	123.8	
					15	6.4	2186 %	120.0	
					20	12.4	4329 %	115.5	
Palmitic acid/ [61.7 °C]	0.17	148.36	Size: 50 μm SA: 46 m^2/g ρ: 300 kg/m^3 Thermal conductivity: 4–100 W/(m·K)	EG was supplied by Fluka Company. EG was obtained through chemical oxidation in a vacuum oven at 65 °C for 24 h.	5	0.24	41 %	–	[10]
					10	0.3	76 %	–	
					15	0.38	124 %	–	
					20	0.6	253 %	–	
Paraffin [62 °C]	0.36		D: 835 μm L: 1846 μm SA: 25.15 m^2/g	EG was supplied from Shanghai Tianmi Industries Co. Lt. EG was obtained by heat treatment in a medium-temperature box resistance furnace.	1	0.59	64 %	207.11	[22]
					3	0.9	150 %	197.22	
					5	1.42	294 %	192.4	
			D: 525 μm L: 1846 μm SA: 28.76 m^2/g		1	0.61	69 %	196.14	
					3	0.93	158 %	187.56	
					5	1.49	314 %	180.71	
			D: 432 μm L: 3050 μm SA: 15.63 m^2/g		1	0.55	53 %	195.06	
					3	0.81	125 %	192.64	
					5	1.37	281 %	187.23	
RT62HC [62.0 °C]	0.202	192.4	D: 20 μm	EG was supplied by Sigratherm Carbon. No further heat treatment was performed on both EG (GFG20 and GFG200) particles as they had already been expanded by the supplier.	2	0.303	50 %	179.1	Data from the Current study
					4	0.424	110 %	175.9	
					6	0.465	130 %	173.6	
			D: 200 μm		2	0.320	58 %	170.5	
					4	0.451	123 %	182.8	
					6	0.518	156 %	173.8	
RT64HC [63.4 °C]	0.221	214.4	D: 20 μm		2	0.317	43 %	202.2	
					4	0.393	78 %	203.5	
					6	0.503	128 %	202.6	
			D:200 μm		2	0.324	46 %	218.2	
					4	0.376	70 %	211.7	
					6	0.442	100 %	206.6	
OM65 [65.7 °C]	0.194	177.3	D: 20 μm		2	0.251	29 %	172.2	
					4	0.369	90 %	168.9	
					6	0.410	111 %	168.9	
			D: 200 μm		2	0.287	48 %	171.7	
					4	0.377	94 %	171.2	
					6	0.428	121 %	164.1	

based on RT62HC with 6 wt% of both 20 μm and 200 μm EG particles.

- Adding EG to PCMs does not impact the phase change temperatures significantly, but there is an uncertainty related to the measurements depending on the accuracy of the experimental equipment.

The utilization of CPCMs in various applications could be further improved through the exploration of the following research recommendations:

- *Advanced Thermal Stability Enhancement*: Investigate innovative methods to enhance the thermal stability of composite phase change materials (CPCMs), focusing on refining processing techniques, optimizing particle size and distribution, and exploring the use of nucleating agents to achieve improved thermal performance and durability.
- *Optimization of EG Mass Fractions*: Deepen investigation by testing additional mass fractions of EG to identify an optimal mass ratio, ensuring optimal thermal properties of CPCMs for various applications.
- *Long-Term Stability Testing*: Extend research by conducting long-term stability testing to assess the durability and reliability of CPCMs over extended periods, providing insights into their performance under real-world conditions and informing practical application scenarios.
- *Exploration of Real-World Applications*: Explore practical applications for CPCMs in various industries and scenarios. Assess integration feasibility and effectiveness of CPCMs into existing systems, providing insights into their potential benefits and practical implementation challenges.
- *Environmental Impact Assessment*: Evaluate the environmental impact of developed CPCMs, considering sustainability and recyclability of materials. Conduct life cycle assessments (LCA) to analyze overall

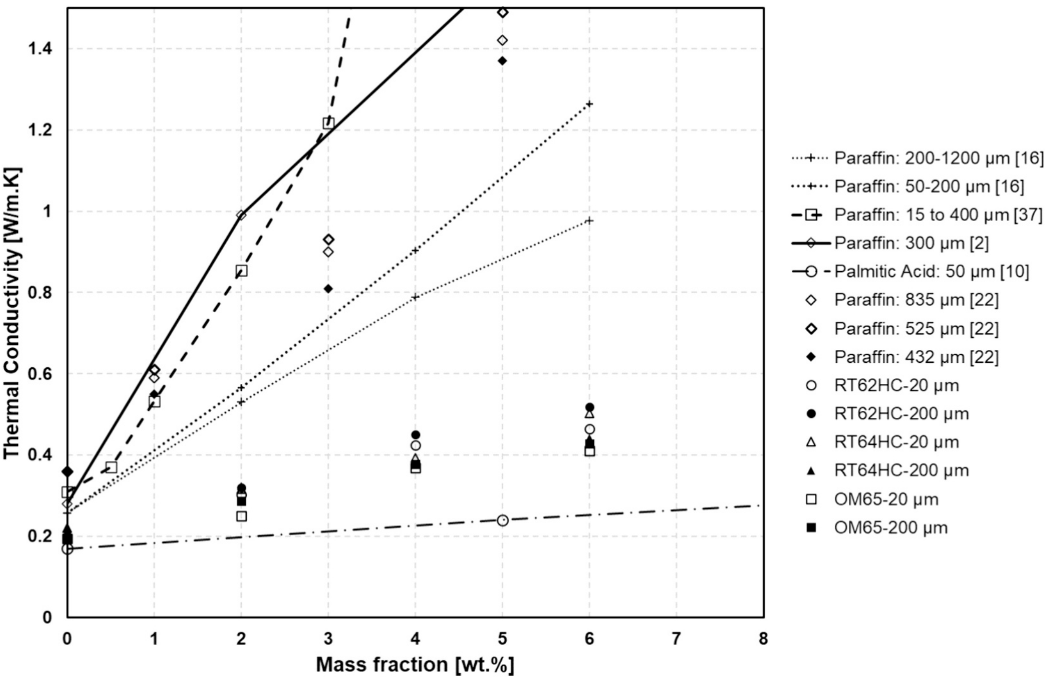

Fig. 11. Comparison of thermal conductivity enhancement vs EG concentration (wt%).

Table 5
Solid thermal conductivity.

Material	wt %	Thermal conductivity [W/(m K)]	Thermal conductivity enhancement [%]	Standard deviation [W/(m·K)]
RT62HC	0	0.202	–	0.004
GFG20	2	0.303	50 %	0.012
	4	0.424	110 %	0.030
	6	0.465	130 %	0.115
GFG200	2	0.320	58 %	0.040
	4	0.451	123 %	0.096
	6	0.518	156 %	0.100
RT64HC	0	0.221	–	0.018
GFG20	2	0.317	43 %	0.021
	4	0.393	78 %	0.035
	6	0.503	128 %	0.057
GFG200	2	0.324	46 %	0.004
	4	0.376	70 %	0.036
	6	0.442	100 %	0.050
OM65	0	0.194	–	0.006
GFG20	2	0.251	29 %	0.023
	4	0.369	90 %	0.052
	6	0.410	111 %	0.065
GFG200	2	0.287	48 %	0.029
	4	0.377	94 %	0.024
	6	0.428	121 %	0.064

environmental implications, guiding the development of eco-friendly CPCMs.

- *Standard Procedures*: Establish standard procedures for measurement thermophysical properties of PCMs reporting uncertainties to reduce discrepancies in the literature.

CRediT authorship contribution statement

Elisangela Jesus D'Oliveira: Writing – original draft, Investigation, Formal analysis, Conceptualization. **Ulugbek Azimov:** Writing – review & editing. **Sol-Carolina Costa Pereira:** Writing – original draft, Validation, Supervision, Project administration, Methodology, Investigation, Funding acquisition, Conceptualization. **Khalid Lafdi:** Writing – review & editing, Supervision.

Table 6
Density variation of CPCMs with the addition of EG.

Material	wt%	Density [kg/m^3]	The difference in density [%]
RT62HC	0	923	–
GFG20	2	943	2
	4	956	4
	6	1010	10
GFG200	2	962	4
	4	976	6
	6	998	8
RT64HC	0	891	3
GFG20	2	931	5
	4	945	7
	6	961	9
GFG200	2	936	6
	4	945	7
	6	964	9
OM65	0	921	2
GFG20	2	962	5
	4	988	7
	6	994	8
GFG200	2	960	4
	4	964	5
	6	955	4

Declaration of competing interest

The authors declare that they have no known competing financial interests or personal relationships that could have appeared to influence the work reported in this paper.

Data availability

Data will be made available on request.

Acknowledgements

This work was supported by the EPSRC Centre for Doctoral Training in Renewable Energy Northeast Universities (ReNU), Project Reference EP/S023826/1. The researchers would also like to thank Linseis and PLUSS advanced technologies.

Appendix A

A.1. Tabulated experimental results

A.1.1. Solid thermal conductivity

Table 5 presents the average measured solid thermal conductivity of the CPCMs with different mass fractions, 2, 4 and 6 wt%, of the two sizes of EG, 20 and 200 μm at room temperature (solid-state — 23 °C) and the percentage of enhancement in thermal conductivity.

A.1.2. Density

Table 6 presents the variation in density of CPCMs with the increase of the mass fraction of the two sizes of EG, 20 and 200 μm.

References

[1] A.F. Regin, S. Solanki, J. Saini, Heat transfer characteristics of thermal energy storage system using PCM capsules: a review, Renew. Sustain. Energy Rev. 12 (9) (2008) 2438–2458.

[2] Q. Wang, D. Zhou, Y. Chen, P. Eames, Z. Wu, Characterization and effects of thermal cycling on the properties of paraffin/expanded graphite composites, Renew. Energy 147 (2020) 1131–1138.

[3] M.F. Demirbas, Thermal energy storage and phase change materials: an overview, Energy Sources B: Econ. Plan. Policy 1 (1) (2006) 85–95.

[4] K. Shank, J. Bernat, E. Regal, J. Leise, X. Ji, S. Tiari, Experimental study of varying heat transfer fluid parameters within a latent heat thermal energy storage system enhanced by fins, Sustainability 14 (14) (2022) 8920.

[5] D. Rozanna, T. Chuah, A. Salmiah, T.S. Choong, M. Sa'Ari, Fatty acids as phase change materials (PCMs) for thermal energy storage: a review, Int. J. Green Energy 1 (4) (2005) 495–513.

[6] A. Sarı, A. Bicer, G. Hekimoğlu, Effects of carbon nanotubes additive on thermal conductivity and thermal energy storage properties of a novel composite phase change material, J. Compos. Mater. 53 (21) (2019) 2967–2980.

[7] A. Sarı, A. Karaipekli, Thermal conductivity and latent heat thermal energy storage characteristics of paraffin/expanded graphite composite as phase change material, Appl. Therm. Eng. 27 (8–9) (2007) 1271–1277.

[8] E.B. Jebasingh, V.A. Arasu, A comprehensive review on latent heat and thermal conductivity of nanoparticle dispersed phase change material for low-temperature applications, Energy Storage Mater. 24 (2020) 52–74.

[9] Q. Ren, F. Meng, P. Guo, A comparative study of PCM melting process in a heat pipe-assisted LHTES unit enhanced with nanoparticles and metal foams by immersed boundary-lattice Boltzmann method at pore-scale, Int. J. Heat Mass Transf. 121 (2018) 1214–1228.

[10] A. Sarı, A. Karaipekli, Preparation, thermal properties and thermal reliability of palmitic acid/expanded graphite composite as form-stable PCM for thermal energy storage, Solar Energy Mater. Solar Cells 93 (5) (2009) 571–576.

[11] W. Cai, W. Yang, Z. Jiang, F. He, K. Zhang, R. He, J. Wu, J. Fan, Numerical and experimental study of paraffin/expanded graphite phase change materials with an anisotropic model, Sol. Energy Mater. Sol. Cells 194 (2019) 111–120.

[12] Z. Zhang, N. Zhang, J. Peng, X. Fang, X. Gao, Y. Fang, Preparation and thermal energy storage properties of paraffin/expanded graphite composite phase change material, Appl. Energy 91 (1) (2012) 426–431.

[13] Y. Lin, Y. Jia, G. Alva, G. Fang, Review on thermal conductivity enhancement, thermal properties and applications of phase change materials in thermal energy storage, Renew. Sustain. Energy Rev. 82 (2018) 2730–2742.

[16] M. Kenisarin, K. Mahkamov, F. Kahwash, I. Makhkamova, Enhancing thermal conductivity of paraffin wax 53–57 °C using expanded graphite, Solar Energy Mater. Solar Cells 200 (2019) 110026.

[17] Z. Zhang, G. Alva, M. Gu, G. Fang, Experimental investigation on n-octadecane/polystyrene/expanded graphite composites as form-stable thermal energy storage materials, Energy 157 (2018) 625–632.

[18] L. Zhao, Q. Yu, M. Li, Y. Zhang, Y. Wang, D. Zhan, S. Jin, Y. Huang, Preparation and thermal properties of low-temperature composite phase-change materials based on a binary eutectic mixture with expanded graphite: effect of particle size and mass fraction, J. Energy Storage 40 (2021) 102778.

[19] Y. Zhao, L. Jin, B. Zou, G. Qiao, T. Zhang, L. Cong, F. Jiang, C. Li, Y. Huang, Y. Ding, Expanded graphite–paraffin composite phase change materials: effect of particle size on the composite structure and properties, Appl. Therm. Eng. 171 (2020) 115015.

[20] B. Lu, Y. Zhang, D. Sun, X. Jing, Experimental investigation on thermal properties of paraffin/expanded graphite composite material for low temperature thermal energy storage, Renew. Energy 178 (2021) 669–678.

[21] X. Wang, B. Li, Z. Qu, J. Zhang, Z. Jin, Effects of graphite microstructure evolution on the anisotropic thermal conductivity of expanded graphite/paraffin phase change materials and their thermal energy storage performance, Int. J. Heat Mass Transf. 155 (2020) 119853.

[22] Z. An, H.J.M. Pea, X. Du, J. Wu, D. Zhang, Preparation and characteristics optimization of octadecanoic acid/octadecanol/expanded graphite based composite phase change materials for energy storage, J. Energy Storage 55 (2022) 105598.

[23] H. Zhang, X. Gao, C. Chen, T. Xu, Y. Fang, Z. Zhang, A capric–palmitic–stearic acid ternary eutectic mixture/expanded graphite composite phase change material for thermal energy storage, Compos. A: Appl. Sci. Manuf. 87 (2016) 138–145.

[24] M. AlMaadeed, S. Labidi, I. Krupa, M. Karkri, Effect of expanded graphite on the phase change materials of high density polyethylene/wax blends, Thermochim. Acta 600 (2015) 35–44.

[25] E.J. D'Oliveira, S.C.C. Pereira, D. Groulx, U. Azimov, Thermophysical properties of nano-enhanced phase change materials for domestic heating applications, J. Energy Storage 46 (2022) 103794.

[26] X. Fang, L.-W. Fan, Q. Ding, X. Wang, X.-L. Yao, J.-F. Hou, Z.-T. Yu, G.-H. Cheng, Y.-C. Hu, K.-F. Cen, Increased thermal conductivity of eicosane-based composite phase change materials in the presence of graphene nanoplatelets, Energy Fuel 27 (7) (2013) 4041–4047.

[27] H. Masoumi, S. Mirfendereski, Modification of physical and thermal characteristics of stearic acid as a phase change materials using TiO_2-nanoparticles, Thermochim. Acta 675 (2019) 9–17.

[28] D. Ezhumalai, G. Sriharan, S. Harikrishnan, Improved thermal energy storage behavior of CuO/palmitic acid composite as phase change material, Mater. Today Proc. 5 (6) (2018) 14618–14627.

[29] L. Müller, G. Rubio-Pérez, A. Bach, N. Muñoz-Rujas, F. Aguilar, J. Worlitschek, Consistent DSC and TGA methodology as basis for the measurement and comparison of thermo-physical properties of phase change materials, Materials 13 (20) (2020) 4486.

[30] L. Feng, J. Wu, W. Sun, W. Cai, Effects of pore structure and pore size of expanded graphite on the properties of paraffin wax/expanded graphite composite phase change materials, Energies 15 (12) (2022) 4201.

[31] Y. Yuan, T. Li, N. Zhang, X. Cao, X. Yang, Investigation on thermal properties of capric–palmitic–stearic acid/activated carbon composite phase change materials for high-temperature cooling application, J. Therm. Anal. Calorim. 124 (2) (2016) 881–888.

[32] D. Zhou, J. Yuan, X. Xiao, Y. Liu, Preparation and characterization of lauric–myristic acid/expanded graphite as composite phase change energy storage material, J. Nanomater. 2021 (2021).

[33] D. Zhou, J. Yuan, Y. Zhou, Y. Liu, Preparation and characterization of myristic acid/expanded graphite composite phase change materials for thermal energy storage, Sci. Rep. 10 (1) (2020) 1–11.

[34] T. Wang, K. Wang, T. Zhang, F. Ye, Z. Liao, C. Xu, Wettability of molten Na_2CO_3–K_2CO_3 on coal fly ash ceramic substrates with expanded graphite, Mater. Chem. Phys. 258 (2021) 123861.

[35] Z. Ling, J. Chen, T. Xu, X. Fang, X. Gao, Z. Zhang, Thermal conductivity of an organic phase change material/expanded graphite composite across the phase change temperature range and a novel thermal conductivity model, Energ. Conver. Manage. 102 (2015) 202–208.

[36] Y. Xin, J. Li, K. Huang, L. Liu, R. Yang, Thermal characteristics enhancement of $Na_2HPO_4{\cdot}12H_2O$/expanded graphite form-stable composite phase change material by the cationic surfactant modification, J. Energy Storage 54 (2022) 105399.

[37] V. Zhelezny, D. Ivchenko, Y. Hlek, O. Khliyeva, K. Shestopalov, Experimental study of phase transition heat of composite thermal energy storage materials paraffin wax/expanded graphite, J. Energy Storage 77 (2024) 110174.

[38] G. Fang, M. Yu, K. Meng, F. Shang, X. Tan, High-performance phase-change materials based on paraffin and expanded graphite for solar thermal energy storage, Energy Fuel 34 (8) (2020) 10109–10119.